ChemComm

Photoelectrochemical Operation of a Surface-Bound, Nickel-Phosphine H2 Evolution Catalyst on p-Si(111): A Molecular Semiconductor|Catalyst Construct

Journal:	*ChemComm*
Manuscript ID:	CC-COM-04-2015-002802.R1
Article Type:	Communication
Date Submitted by the Author:	04-May-2015
Complete List of Authors:	Seo, Junhyeok; The University of Texas at Austin, Department of Chemistry Pekarek, Ryan; The University of Texas at Austin, Department of Chemistry Rose, Michael; The University of Texas at Austin,

Cite this: DOI: 10.1039/c0xx00000x

www.rsc.org/xxxxxx

ARTICLE TYPE

Photoelectrochemical Operation of a Surface-Bound, Nickel-Phosphine H_2 Evolution Catalyst on *p*-Si(111): A Molecular Semiconductor|Catalyst Construct

Junhyeok Seo, Ryan T. Pekarek and Michael J. Rose*

Received (in XXX, XXX) Xth XXXXXXXXX 20XX, Accepted Xth XXXXXXXXX 20XX
DOI: 10.1039/b000000x

We demonstrate the covalent attachment and catalytic function of a nickel-phosphine H_2 evolution catalyst to a *p*-Si(111) photoelectrode. The covalently assembled semiconductor|molecular construct achieves a synergistic improvement (ΔV_{onset} = +200 mV) as compared to a solution of $[(PNP)_2Ni]^{2+}$ in contact with a *p*-Si(111)–CH_3 photoelectrode.

The integration of molecular catalysts with light-absorbers (semiconductors) remains at the pinnacle of challenges facing the molecular catalysis branch of solar fuels research.[1-4] Additionally, retaining the earth abundant nature of each component is essential to promoting the feasibility and widespread application of such a device. Silicon is an excellent candidate as a putative light absorber in a parallel or tandem system,[5] due to its ideal band gap (E_g = 1.12 eV) for the absorption of low energy sunlight to drive the $2H^+ \rightarrow H_2$ conversion.[6] In the arena of molecular catalysts, *p*-type silicon has been used as a photocathode with free catalysts in solution,[7,8] and silicon also shows great promise due to developing coupling methods to covalently attach molecular species to fully passivated surfaces.[9-11] In this regime, the Si(111) surface presents one particular advantage over the Si(100) orientation used in most materials-based approaches: the rigidly perpendicular orientation of Si–X bonds on Si(111) renders it uniquely suited for molecular modification. However, its need for extreme bonding regularity (to prevent surface defect sites) requires molecular passivation – typically by methylation.[12]

In the last decade, the development of molecular catalysts for electrochemical dihydrogen (H_2) generation has blossomed and matured. The families of Co/Fe tetraimines investigated by Artero and Fontecave,[13] Peters[14] and others[15-17] – as well as the nickel phosphines developed by DuBois and Bullock[18] have achieved remarkable operating parameters (TOF > 100,000 s^{-1}, Ni-phosphines;[18] E_{cat} = –50 to –200 mV vs NHE, Co-N4 complexes[19,20]). Indeed, a multitude of researchers have grafted derivative of these catalysts onto electrochemically active substrates such as glassy carbon,[21,22] HOPG,[23] ITO,[24] graphene,[25] and carbon nanotubes.[26] However, the challenge of incorporating such catalysts onto *photo*-electrochemically active substrates remains open.[11,27] In this work, we report that covalent attachment of a DuBois-type PNP Ni catalyst (substituted with phenyl units substituent on phosphine and amine)[28] to a *p*-Si(111) substrate affords H_2 generation from the surface-bound catalyst.

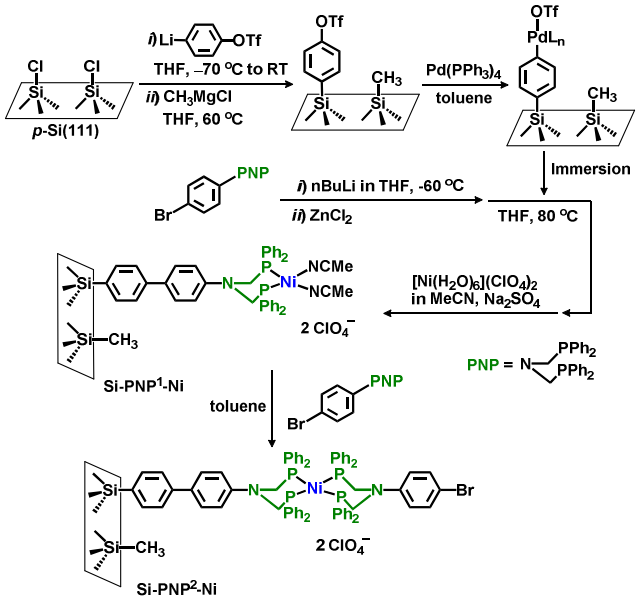

Scheme 1. Synthetic approach to functionalization of *p*-Si(111)–Cl substrates[29] with molecular linkers: Negishi coupling of catalyst ligand to surface linker, metalation with nickel(II) source, and capping with an exogenous PNP ligand.

We first devised a surface linker that would be amenable to selective lithiation (for attachment), while retaining a second functional group to participate in Pd-catalyzed coupling reaction. The *para* bromo- and triflato- functional groups on a phenyl unit were ideal in this regard. A lithiated linker was generated via treatment of *para*-triflatobromobenzene with 0.9 equiv of *n*-BuLi in THF at –70 °C for 1 h. The selective Br site lithiation and the persistence of the –OTf group was confirmed by H_2O quench and subsequent analysis by ^1H and ^{19}F NMR spectroscopy (^1H: δ = 7.46 (t 2H), 7.40 (d 1H), 7.28 (d 2H) ppm; ^{19}F: –72.93 ppm in $CDCl_3$) and MS (*m*/*z* = 226.9987, no Br isotope pattern). The *p*-Si(111)–Cl substrate[29] was then incubated with the lithiate in THF from –70 °C → RT. To further passivate the surface and prevent the formation of electronic defect sites, the remaining Si(111)–Cl sites were methylated according to the reported procedure (CH_3MgCl, THF, 60 °C) by Lewis et al.[29] XPS analysis for the F 1*s* region indicated θ_{OTf} = 21.8±1.0% coverage of the

linker (all coverages herein are stated per atop Si site, Table 1).

To promote coupling of the PNP ligand (PNP = $Ph_2PCH_2NCH_2PPh_2$), the triflate group was activated by treatment of the surface with a dilute solution of $[Pd(PPh_3)_4]$ in toluene at room temperature,[9] thus generating the surface-bound organometallic Pd^{II} intermediate.[9] In a separate vessel, $Br(C_6H_4)PNP$[30] was lithiated with *n*-BuLi at −60 °C in THF and $ZnCl_2$ was reacted with the lithiate at room temperature (Scheme 1). The activated Pd^{II}-bound sample was then immersed in the solution of the ZnCl-adduct, and the solution heated at 80 °C for 4 h. The resulting surface was rinsed and sonicated thoroughly in THF to remove any adventitious entities (carbon, $MgCl_2$, etc.). The coupling reaction thus generated the ligand-modified surface as evidenced by the new N 1*s* XPS signal (θ_N = 21.2±6.8%, Fig. 1c), the diminished triflato-F 1*s* feature (θ_{OTf} = 5.5±2.0% at 688.1 eV, Fig. 1b), and subsequent metalation studies (vide infra). Some remaining inorganic F was also detected at 684.5 eV (Fig. 1b).

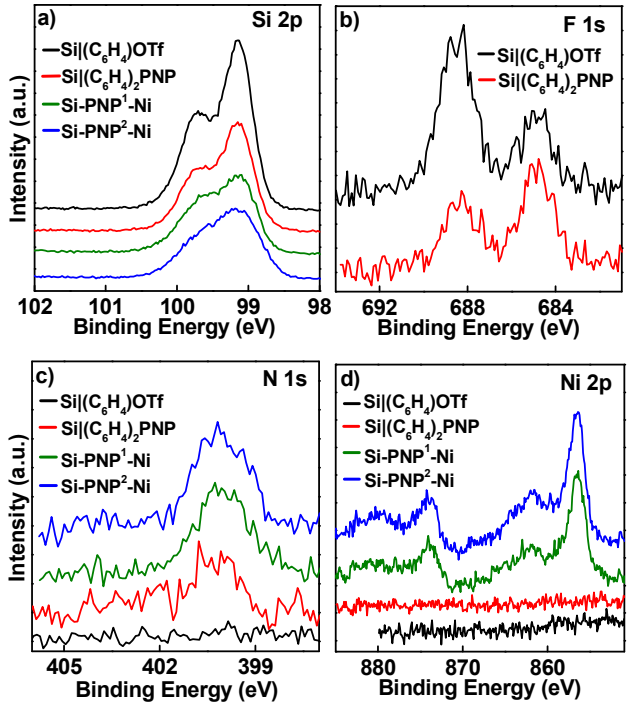

Fig. 1 High resolution XPS spectra of (*a*) Si 2*p*, (*b*) F 1*s*, (*c*) N 1*s*, and (*d*) Ni 2*p* for the following surfaces: $Si|(C_6H_4)OTf$ (black), $Si|(C_6H_4)_2PNP$ (red), Si-PNP[1]–Ni (green), and Si-PNP[2]–Ni (blue). *Data collection*: Si 2*p*, F 1*s*, N 1*s*, Ni 2*p*: t_{dwell} = 1200, 2000, 4800, 4800 ms (respectively).

Interestingly, metalation of the $Si|(C_6H_4)_2PNP$ interface could be achieved only under specific conditions. For example, treatment of the $Si|(C_6H_4)_2PNP$ surface with $[Ni(H_2O)_6](X)_2$ (X = BF_4, ClO_4) in MeCN did not lead to any nickel incorporation, as judged by the Ni 2*p* XPS signal. However, drying the nickel-containing MeCN solution with Na_2SO_4 for several hours prior to metalation did effect metalation of the $Si|(C_6H_4)_2PNP$ surface (θ_{Ni} = 24.6±0.8%, θ_N = 59.3±13.4%, Fig. 1c and 1d). In contrast, treatment of the $Si(111)|(C_6H_4)OTf$ surface with the same nickel(II) solution did not result in any significant incorporation of nickel (θ_{Ni} < 0.5%). Intriguingly, re-treatment of the metalated surface with 'wet' MeCN (0.1 % H_2O for 1 h) did not abstract the surface-bound Ni, indicating the kinetic stability of the surface-bound $Si|(C_6H_4)_2PNP\text{-}Ni(MeCN)_2$ (= Si-PNP[1]-Ni) moiety. Also, the metallation did not alter the surface recombination velocity (SRV, Table 1), indicating a simple binding event at the surface – i.e. no deposition of Ni^0 (also evidenced by XPS binding energy eV values). Overall, the observed coordination chemistry conditions required for metalation reinforce the notion of the molecular nature of the PNP-Ni^{II} interaction.

Table 1. High resolution XPS quantification[a] (% atop sites) of each element coverage (or functional group, OTf) determined for the indicated Si substrates; (right) surface recombination velocities (*S*).

Substrate	OTf (F) (%)	N (%)	Ni (%)	SRV (*S*) (cm s^{-1})
$Si|(C_6H_4)OTf$	21.8±1.0	< 0.5	< 0.5	1372±29.8
$Si|(C_6H_4)_2PNP$	5.5±2.0	21.2±6.8	< 0.5	2415±26.2
Si-PNP[1]-Ni	6.9±2.5	59.3±13.4	24.6±0.8	2395±26.3
Si-PNP[2]-Ni	9.7±2.9	41.9±4.9	19.1±5.7	2547±46.3
Si-PNP[2]-Ni[b]	4.98	26.2	15.6	1636

[a] Values (%) normalized to the Si 2*p* peak area; [b] After 30 cycles of PEC-CV scans in 0.2 M $LiClO_4$ (MeCN), 0.1 V/s, broadband LED light 33 mW cm^{-2}.

To further demonstrate covalent attachment and electronic communication of the PNP-$Ni(MeCN)_2$ moiety, photoelectrochemical studies were pursued. The cyclic voltammogram (CV, Fig. 2) of the integrated Si-PNP[1]-Ni photocathode was obtained in MeCN electrolyte under N_2 atmosphere (glove box) illuminated conditions (broadband LED 33 mW cm^{-2}; *note*: the current was not light-limited under any tested condition). The primary cathodic features are observed at −0.22 V vs NHE (all potentials referenced to Fc/Fc^+ as internal standard, then converted to NHE by adding 0.626 V). The increase of current in the cathodic wave at −0.22 V vs NHE corresponds to the Ni(II/I) conversion ($E_{1/2}$ for Ni(II/I) = −0.215 V vs NHE), and the feature exhibits a linear scan rate dependence (Fig. 2a, Inset). Assignment of another reduction behavior of Ni(I/0)[28] is ambiguous due to the overlap with a cathodic wave that appears on the control Si–CH_3 surface. (Fig. S1, supporting information).

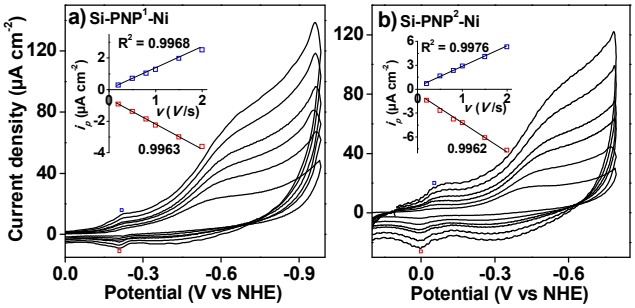

Fig. 2 CV traces of two catalyst-modified substrates: (*a*) Si-PNP[1]-Ni, and (*b*) Si-PNP[2]-Ni. *Inset:* Scan-rate dependence for (*a*) and (*b*). *Experiment conditions:* N_2 atmosphere (glove box), MeCN, 0.2 M $LiClO_4$, broadband LED 33 mW cm^{-2}.

To demonstrate the molecular nature of the redox couple – and to investigate the local coordination environment – the surface was separately treated with excess PNP ligand in toluene for 1 h, then washed thoroughly with toluene and THF. First, it is noteworthy that the surface nickel was not abstracted by the PNP ligand in solution, again demonstrating the kinetic stability of the

metalated surface. XPS analysis of the resulting surface generated an N 1*s* feature roughly in a $^2/_3$ ratio (θ_N = 41.9±4.9%) of the original metalated surface (*p*-Si(111)|$(C_6H_4)_2$PNP-Ni$(MeCN)_2$, θ_N = 59.3±13.4%), indicating incorporation of a second equivalent of PNP ligand (and loss of two MeCN ligands) to the surface coordination environment. Additionally, the CV of the modified *p*-Si(111)|$(C_6H_4)_2$PNP-Ni-PNP(C_6H_4)Br/$(ClO_4)_2$ (= Si-PNP^2-Ni) surface exhibits a redox feature that is anodically shifted by 0.18 V ($E_{1/2}$ for Ni(II/I) = –0.03 V vs NHE) to –0.04 V vs NHE. Such a result is expected based on the more facile access to the Ni(II/I) oxidation states in a softer P4-Ni^{II} coordination environment versus the P2/N2-Ni^{II} ligand set.[19] The Si-PNP^2-Ni surface also exhibits a linear scan rate dependence (Fig. 2b, inset), indicative of the non-diffusive nature of the redox species. The covalently attached Ni coverage in the Si-PNP^2-Ni surface was determined by Ni 2*p* XPS data as 19.1±5.7% (Table 1). In previous work by others involving attachment of potential catalysts to Si(111), a fast loss of Rh was observed during several CV cycles.[11] Importantly, in this case the XPS data of the Si-PNP^2-Ni sample after consecutive PEC-CV scans (30 cycles between –0.3 to –1.6 V *vs* $Fc^{+/0}$) revealed only a minor decrease (not statistically significant) in the Ni 2*p* coverage (θ_{Ni} = 15.6%, Table 1).

To demonstrate the catalytic function of the immobilized Ni$(PNP)_n$ surfaces, cathodic CVs were obtained in the presence of increasing concentrations of trifluoroacetic acid (TFA) in MeCN under N_2 (glove box). The resulting *J-V* traces of Si-PNP^2-Ni and Si-PNP^1-Ni show a similar shape (Fig. 3a and Fig. S2, respectively), and both samples demonstrate the characteristic increase in current. The current increase correlates with the generation of H_2 gas, which was confirmed by GC-MS analysis of the cell headspace in a controlled potential electrolysis (see experimental details in SI). The V_{onset} of the Si-PNP^2-Ni sample was noted at –0.06 V vs NHE, and the V_{onset} = –0.09 V of the Si-PNP^1-Ni (where V_{onset} = *E* for 0.05 mA cm^{-2}; for comparison, variation of the V_{onset} threshold definition is plotted in Fig. S3, SI). The turnover frequency (TOF) of the Si-PNP^2-Ni sample was calculated as 285 s^{-1} from *j* (A cm^{-2}) using 91 mM TFA at –0.67 V by an equation of TOF = j/nFN, where *n* is the stoichiometric number of electrons consumed in the reaction (*n* = 2), *F* is Faraday constant, *N* is the number of catalytic species. The amount of the confined Ni$(PNP)_2$ catalyst was determined to be 2.5 × 10^{-10} mol cm^{-2} (~19.1% coverage on Si(111) surface, where atop silicon ~1.3 × 10^{-9} mol cm^{-2})[31]. The acid dependence of the catalytic activity (J_{max} vs [TFA]; Inset of Fig. 3a and Fig. S2) saturates for each sample near [TFA] = 90 mM. As a control experiment, the *J-V* curves for the corresponding substrate in the *absence of Ni ion* (V_{onset} of *p*-Si(111)|CH_3 = –0.14 V vs NHE, Fig. 3C (green line) and Fig. S4 in SI) indicate that Ni is responsible for the anodic shift of V_{onset}. Additionally, Pt nanoparticles (ALD deposition) on the *p*-Si(111)|CH_3 (Fig. 3b) showed about 0.04 V more positive V_{onset} (= –0.02 V vs NHE) than the attached Si-PNP^2-Ni sample. Once a suitably negative potential was applied (< ~ –0.3 vs NHE), the *p*-Si(111)|CH_3|Pt sample showed the fastest current increase, but the rise-to-max occurred relatively slowly in the low reduction potential range > –0.3 V (Fig. 3c). These results are comparable with a previous observation in an aqueous solution, wherein the *p*-Si(111)|CH_3|Pt surface exhibited a sharper ΔV (V_{onset} – V_{Jmax}) than the *p*-Si(111)|CH_3 surface by 0.08 V.[32] The effect of the insulating methyl group on the Si surface seems to be dominant in the low reduction potential region. In contrast, the Ni$(PNP)_n$ catalyst, directly connected to Si through the phenyl ring, exhibited a comparatively rapid current increase near –0.3 V vs NHE. The overpotential of Si-PNP^2-Ni was calculated as 0.34 V for 15.6 mM TFA (thermodynamic potential E^0_{TFA} = –0.34 V vs $Fc^{+/0}$ using Pt wire WE).

Lastly, as a control experiment we also investigated the photoelectrochemical behavior of the dissolved $[Ni(PNP(C_6H_4)Br)_2]^{2+}$ complex generated in situ (2 μM in MeCN), while using a *p*-Si(111)|CH_3 working electrode. Interestingly, the non-attached catalyst $[Ni(PNP(C_6H_4)Br)_2]^{2+}$ (dashed line in Fig. 3d), exhibited a more negative V_{onset} value of –0.26 V vs NHE – about 0.2 V more negative potential than the Si-PNP^2-Ni construct – despite its electron-withdrawing *p*-bromo substituents. Thus, the semiconductor|catalyst construct exhibits a synergistic catalytic function that is greater than the 'the sum of the parts', as might be expected. The enhanced performance may also be due to expedited electron transfer to the Ni$(PNP)_2$ moiety by the conjugated (and covalent) phenyl linker.

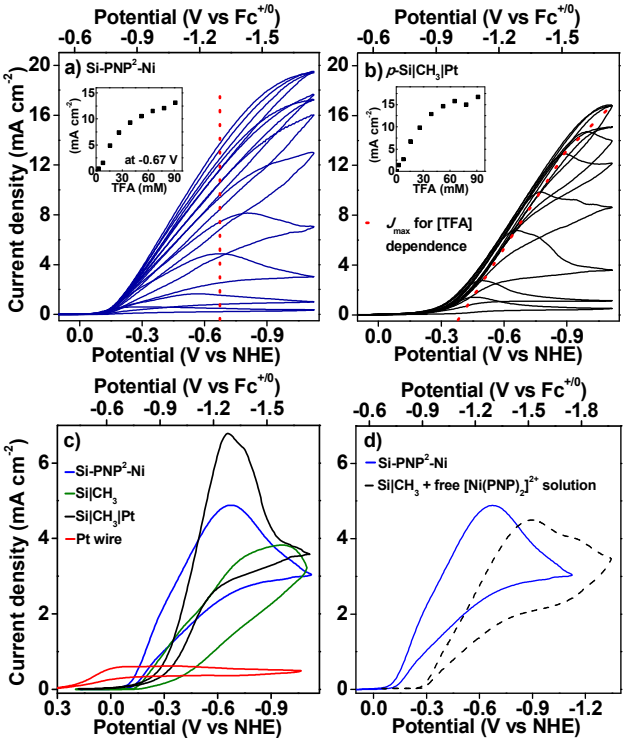

Fig. 3 Catalytic CVs of functionalized substrates: (*a*) Si-PNP^2-Ni (blue); (*b*) *p*-Si(111)|CH_3|Pt control (black); (*c*) comparison of (*a*), (*b*), *p*-Si(111)|CH_3 (green) samples, and Pt wire WE (red) at 15.6 mM TFA; (*d*) comparison of Si-PNP^2-Ni (blue) and 2 μM $[Ni(PNP(C_6H_4)Br)_2](ClO_4)_2$ solution on the Si(111)|CH_3 surface (dashed). *Insets:* (*a*) [TFA] dependence at –0.67 V vs NHE; (*b*) [TFA] dependence at the indicated (red dashed line) potentials of J_{max}. *Experiment conditions:* N_2 atmosphere (glove box), 0.2 M $LiClO_4$ (MeCN), broadband LED 33 mW cm^{-2}, 100 mV s^{-1} scan rate.

In closing, we have demonstrated the photo-electrochemical operation of a functional, molecular catalyst to a passivated Si surface. The earth abundance of the semiconductor (Si) and catalyst (Ni) is of particular note. The resulting Ni complex exhibits excellent stability during PEC-CV measurements in

$MeCN/LiClO_4$ electrolyte. Additionally, the present construct provides a catalytic rate (TOF = ~ 285 s^{-1}) and resulting current (~20 mA cm^{-2}) that is commensurate with that expected of 1-sun illumination on Si (~25 mA cm^{-2}). Ongoing work is focused on modulation of the band-edge position,[32] and higher catalytic turnover (by ligand selection) of the catalyst-functionalized substrate for improved solar→H_2 efficiency.

Notes and references

Department of Chemistry, The University of Texas at Austin, Austin, Texas 78712, United States. Fax: +1 512 471-6835; Tel: +1 512 471-4456; E-mail: mrose@cm.utexas.edu

† Electronic Supplementary Information (ESI) available: Procedures for Si etching, molecule attachments; PEC-CV figures; V_{onset} definition are included. See DOI: 10.1039/b000000x/

1 M. A. Modestino, K. A. Walczak, A. Berger, C. M. Evans, S. Haussener, C. Koval, J. S. Newman, J. W. Ager, R. A. Segalman, *Energy Environ. Sci.* 2014, **7**, 297.

2 X. Chen, S. Shen, L. Guo, S. S. Mao, *Chem. Rev.* 2010, **110**, 6503.

3 S. Y. Reece, J. A. Hamel, K. Sung, T. D. Jarvi, A. J. Esswein, J. J. H. Pijpers, D. G. Nocera, *Science* 2011, **334**, 645.

4 C. A. Rodriguez, M. A. Modestino, D. Psaltis, C. Moser, *Energy Environ. Sci.* 2014, **7**, 3828.

5 Y. Hou, B. L. Abrams, P. C. K. Vesborg, M. E. Björketun, K. Herbst, L. Bech, A. M. Setti, C. D. Damsgaard, T. Pedersen, O. Hansen, J. Rossmeisl, S. Dahl, J. K. Nørskov, I. Chorkendorff, *Nat. Mater.* 2011, **10**, 434.

6 M. G. Walter, E. L. Warren, J. R. McKone, S. W. Boettcher, Q. Mi, E. A. Santori, N. S. Lewis, *Chem. Rev.* 2010, **110**, 6446.

7 B. Kumar, M. Beyler, C. P. Kubiak, S. Ott, *Chem. Eur. J.* 2012, **18**, 1295.

8 B. Kumar, J. M. Smieja, C. P. Kubiak, *J. Phys. Chem. C* 2010, **114**, 14220.

9 L. E. O'Leary, M. J. Rose, T. X. Ding, E. Johansson, B. S. Brunschwig, N. S. Lewis, *J. Am. Chem. Soc.* 2013, **135**, 10081.

10 G. F. Moore, I. D. Sharp, *J. Phys. Chem. Lett.* 2013, **4**, 568.

11 J. R. C. Lattimer, J. D. Blakemore, W. Sattler, S. Gul, R. Chatterjee, V. K. Yachandra, J. Yano, B. S. Brunschwig, N. S. Lewis, H. B. Gray, *Dalton Trans.* 2014, **43**, 15004.

12 K. T. Wong, N. S. Lewis, *Acc. Chem. Res.* 2014, **47**, 3037.

13 P.-A. Jacques, V. Artero, J. Pécaut, M. Fontecave, *Proc. Natl. Acad. Sci. USA.* 2009, **106**, 20627.

14 X. Hu, B. S. Brunschwig, J. C. Peters, *J. Am. Chem. Soc.* 2007, **129**, 8988.

15 F. Lakadamyali, M. Kato, N. M. Muresan, E. Reisner, *Angew. Chem. Int. Ed.* 2012, **51**, 9381.

16 J. L. Dempsey, B. S. Brunschwig, J. R. Winkler, H. B. Gray, *Acc. Chem. Res.* 2009, **42**, 1995.

17 P. Connolly, J. H. Espenson, *Inorg. Chem.* 1986, **25**, 2684.

18 M. L. Helm, M. P. Stewart, R. M. Bullock, M. R. DuBois, D. L. DuBois, *Science* 2011, **333**, 863.

19 G. M. Jacobsen, J. Y. Yang, B. Twamley, A. D. Wilson, R. M. Bullock, M. Rakowski DuBois, D. L. DuBois, *Energy Environ. Sci.* 2008, **1**, 167.

20 E. S. Wiedner, J. Y. Yang, W. G. Dougherty, W. S. Kassel, R. M. Bullock, M. R. DuBois, D. L. DuBois, *Organometallics* 2010, **29**, 5390.

21 A. K. Das, M. H. Engelhard, R. M. Bullock, J. A. S. Roberts, *Inorg. Chem.* 2014, **53**, 6875.

22 L. A. Berben, J. C. Peters, *Chem. Commun.,* 2010, **46**, 398.

23 G. M. Swain, *J. Electrochem. Soc.,* 1994, **141**, 3382.

24 N. M. Muresan, J. Willkomm, D. Mersch, Y. Vaynzof, E. Reisner, *Angew. Chem. Int. Ed.* 2012, **51**, 12749.

25 S. C. Eady, S. L. Peczonczyk, S. Maldonado, N. Lehnert, *Chem. Commun.,* 2014, **50**, 8065.

26 A. Le Goff, V. Artero, B. Jousselme, P. D. Tran, N. Guillet, R. Métayé, A. Fihri, S. Palacin, M. Fontecave, *Science* 2009, **326**, 1384.

27 A. Krawicz, J. Yang, E. Anzenberg, J. Yano, I. D. Sharp, G. F. Moore, *J. Am. Chem. Soc.* 2013, **135**, 11861.

28 C. J. Curtis, A. Miedaner, R. Ciancanelli, W. W. Ellis, B. C. Noll, M. Rakowski DuBois, D. L. DuBois, *Inorg. Chem.* 2003, **42**, 216.

29 A. Bansal, X. Li, I. Lauermann, N. S. Lewis, S. I. Yi, W. H. Weinberg, *J. Am. Chem. Soc.* 1996, **118**, 7225.

30 S. E. Durran, M. R. J. Elsegood, N. Hawkins, M. B. Smith, S. Talib, *Tetrahedron Lett.* 2003, **44**, 5255.

31 E. J. Nemanick, P. T. Hurley, B. S. Brunschwig, N. S. Lewis, *J. Phys. Chem. B* 2006, **110**, 14800.

32 J. Seo, H. J. Kim, R. T. Pekarek, M. J. Rose, *J. Am. Chem. Soc.* 2015, **137**, 3173.